Determination of the Cs_2 $0_g^-(P_{3/2})$ potential curve and of Cs $6P_{1/2,3/2}$ atomic radiative lifetimes from photoassociation spectroscopy

C. Amiot, O. Dulieu, R. F. Gutterres, and F. Masnou-Seeuws
Laboratoire Aimé Cotton, CNRS, Bâtiment 505, Campus d'Orsay 91405, Orsay Cedex, France
(Received 16 July 2002; published 21 November 2002)

An analytical expression for the external well of the Cs_2 $0_g^-(6s+6P_{3/2})$ double-well potential curve is derived, involving asymptotic parameters fitted on the spectrum obtained from photoassociation of ultracold cesium atoms and ultracold molecule formation [Fioretti *et al.*, Europhys. J. D **5**, 389 (1999)]. The results are compared to a previous Rydberg-Klein-Rees determination from our group, and may have consequences on the determination of cesium triplet scattering length. Values for radiative lifetimes $\tau_{3/2}=30.462(3)$ ns and $\tau_{1/2}=34.88(2)$ ns of the $6P_{3/2}$ and $6P_{1/2}$ atomic levels, respectively, are extracted with an accuracy better than previous determinations. The method of Derevianko and Porsev [Phys. Rev. A **65**, 053403 (2002)], allows the derivation of an improved value for the van der Waals coefficient of ground-state cesium molecule, $C_6^{6s}=6828(19)$ a.u.

DOI: 10.1103/PhysRevA.66.052506 PACS number(s): 32.10.Dk, 32.70.Cs

I. INTRODUCTION

The observation of translationally ultracold molecules ($T \leqslant 10^{-3}$ *K*), formed by photoassociation (PA) of trapped cold atoms and stabilized by spontaneous emission, has been demonstrated for Cs_2 [1], K_2 [2], and Rb_2 [3], opening the way to the achievement of large and dense samples of ultracold molecules. In the photoassociation step, a pair of cold alkali atoms, mainly at large interatomic distance, absorbs a photon with a frequency red-detuned from the lowest $s \rightarrow p$ atomic transition frequency. A short-lived molecule is thus created, most often in a high-lying rovibrational level of an excited electronic state, correlated to the first $s+p$ dissociation limit. The corresponding radial motion extends up to internuclear distances R which can exceed $100a_0$, in a region where the two atoms interact mainly through the C_3/R^3 long-range dipole-dipole interaction. The formation of long-lived ultracold molecules relies on the possibility for the excited molecular level to decay towards rovibrational levels of the molecular ground state or lowest (metastable) triplet state.

In the cesium and rubidium experiments quoted above, the double-well structure of the long-range 0_g^- molecular state correlated to the $nS+nP_{3/2}$ dissociation limit ($n=5$ and 6 for Rb and Cs, respectively) is a key feature in the cold molecule formation process. Hereafter, this state will be labeled as $0_g^-(P_{3/2})$. The PA process is favored by the large extension of the vibrational motion in the external well, while the barrier between the two wells enhances the radial probability density at intermediate distances, where the spontaneous decay of the photoassociated level towards bound levels of the lowest triplet electronic state $a^3\Sigma_u^+$ is efficient. The long-lived molecules are then photoionized into molecular ions, providing a very efficient method for the detection of ultracold molecules, with a signal-to-noise ratio better than in trap-loss measurements [4]. The detection of such ions as a function of the detuning of the PA laser provides spectroscopy data with an accuracy of about 0.005 cm^{-1} [1].

The external well of the $0_g^-(P_{3/2})$ double-well curve in alkali dimers belonging to the class of pure long-range molecular states first described by Stwalley *et al.* [5] is almost entirely located within the asymptotic region, where the chemical exchange energy contribution is weak enough to be treated as a perturbation. The shape of this well is mainly determined by asymptotic atom-atom interaction, which can be evaluated analytically through multipole expansion. The leading term is the dipole-dipole C_3/R^3 potential, where the C_3 coefficient is proportional to the square of the electric dipole matrix element for the $6P_{3/2} \rightarrow 6S_{1/2}$ transition. The analysis of the $0_g^-(P_{3/2})$ spectra has been already achieved in several PA experiments as a powerful method to extract accurate data. In particular, the high precision of PA spectroscopy has allowed the determination of the C_3 coefficient and hence of the atomic radiative lifetime of the first-excited p state in Li [6], Na [7], and K [8]. The uncertainty on the lifetime is in the 0.1–0.2 % range (0.03% for Li), similar to, or better than, the one obtained in most atomic spectroscopy experiments [9]. For a while, it seemed that despite the gain in accuracy from molecular ion detection, the same precision could not be reached for the heavier alkalis [10], where the large value of the fine structure prevents such an analysis. Recent work on rubidium [11] opens the way beyond this limitation.

Obtaining the same level of accuracy for cesium is therefore a challenge. Indeed, the latter atom has been preferentially used for measurements of atomic parity nonconservation [12,13], which provides a test of the standard model in elementary particles. Knowledge of the electric dipole matrix element for the $6P_{1/2} \rightarrow 6S_{1/2}$ transition is essential for the interpretation of such experiments, and recently Derevianko and Porsev [10] derived this quantity from the van der Waals coefficient C_6^{6s} of the ground state, fitted on ultracold collision data [14]. The aim of the present paper is to show that a fit of photoassociation spectroscopy data does lead to a determination of the electric dipole matrix elements for both $6P_{3/2} \rightarrow 6S_{1/2}$ and $6P_{1/2} \rightarrow 6S_{1/2}$ transitions with a precision beyond the 0.1% level.

Besides, the $0_g^-(P_{3/2})$ state is responsible for the most extended PA spectrum obtained in the cesium experiment

[15], showing intensity minima that are associated to the nodal structure of the initial continuum wave function of the colliding cold atoms, interacting through the $a^3\Sigma_u^+$ state. Their interpretation is therefore of utmost importance in the determination of the triplet scattering length [16], which is a key datum in the modeling of Bose-Einstein condensates.

In a previous paper [15], herafter called paper I, we determined a potential curve for the $0_g^-(P_{3/2})$ external potential well from cesium PA data, using the standard Rydberg-Klein-Rees (RKR) procedure with a near-dissociation expansion (NDE). Energy levels and rotational constants calculated from the RKR curve were very satisfactory, but we were not able to extract an accurate value for the C_3 coefficient—which varied by up to 10% according to the chosen fitting procedure—and hence neither for the atomic radiative lifetime. Indeed, the RKR curve did not display correct physical behavior with the peculiar feature of the $0_g^-(P_{3/2})$ external potential well where, due to an avoided crossing, the shape is dominated by a R^{-3} variation both in the repulsive inner branch and in the long-range attractive branch. The standard RKR fitting procedure, well adapted to the usual short-range exponential behavior of most molecular potentials, is not sufficient when there is a marked correlation between the shapes of the inner and outer branches.

Therefore, in the present paper, we derive an analytical representation for the $0_g^-(P_{3/2})$ external potential well in Cs_2, based on an asymptotic expansion involving parameters fitted on the experimental PA spectrum from paper I. The comparison with our previous analysis using RKR procedure [15] is presented, having in mind the consequences for the determination of the scattering length from the intensity minima in the PA spectrum. We show that in contrast with the RKR analysis, new values for the radiative lifetime of the $6p\ ^2P_{3/2}$ and $6p\ ^2P_{1/2}$ atomic levels can be obtained. Our analysis illustrates the striking differences that can exist between two potentials obtained by equally accurate procedures for the inversion of experimental data.

II. THE REPRESENTATION OF THE Cs_2 $0_g^-(P_{3/2})$ EXTERNAL WELL

In order to represent the energy levels lying within the external well of the $0_g^-(P_{3/2})$ state in Cs_2, we closely follow the approach used in the recent work on Rb_2 [11], based on the asymptotic description of atom-atom interactions.

In Hund's case-*c* representation, the $0_g^-(P_{3/2})$ double-well state arises from the mixing between the $^3\Sigma_g^+(6s+6p)$ and $^3\Pi_g(6s+6p)$ Hund's case-*a* states, which respectively are attractive and repulsive at large internuclear distances. They are coupled through the spin-orbit interaction according to the electronic Hamiltonian

$$H=\begin{pmatrix} V^{\Pi}(R)-\Delta^{\Pi\Pi}(R) & \Delta^{\Sigma\Pi}(R) \\ \Delta^{\Sigma\Pi}(R) & V^{\Sigma}(R) \end{pmatrix}, \tag{1}$$

where $V^{\Pi}(R)$ and $(V^{\Sigma}(R))$ are the $^3\Pi_g$ and $(^3\Sigma_g^+)$ potentials, and $\Delta^{\Pi\Pi}(R)$ and $\Delta^{\Sigma\Pi}(R)$ are the *R*-dependent spin-orbit interaction within the $^3\Pi_g$ manifold and between the $^3\Pi_g$ and $^3\Sigma_g^+$ states, respectively.

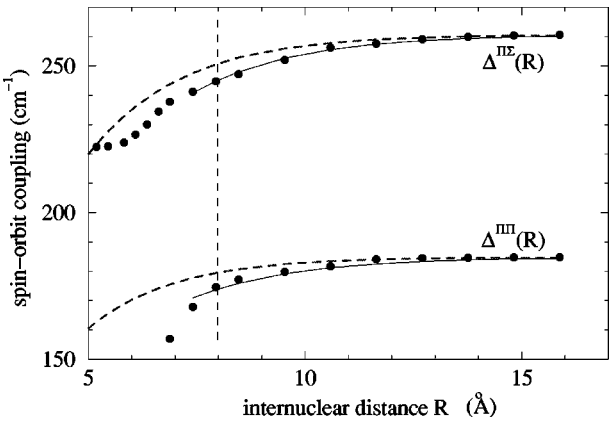

FIG. 1. Variation of the spin-orbit matrix element coupling the $^3\Pi_g$ and $^3\Sigma_g^+$ states. Closed circles: from quantum chemistry calculations [19]. Full line: fit of the quantum chemistry calculations with Eq. (5). Dashed line: result from the fitting of experimental energy levels. Vertical dashed line: the limit beyond which we use the parametrization of Eq. (5).

It is known from previous studies [15] that the $0_g^-(P_{3/2})$ external well is located beyond $15a_0$, with a minimum around $25a_0$, while the LeRoy criterion [17] yields a distance of $R_{LR}\approx 28.5a_0$, beyond which an asymptotic description of the potential is reliable. In other words, for the $0_g^-(P_{3/2})$ state the Cs_2 molecule is not a pure long-range molecule as defined by Stwalley and co-workers [5]. Nevertheless, we assume here that the exchange interaction acts as a perturbation, and write the potential energies according to the well-known multipole expansion:

$$V^{\Sigma/\Pi}=-\frac{C_3^{\Sigma/\Pi}}{R^3}-\frac{C_6^{\Sigma/\Pi}}{R^6}-\frac{C_8^{\Sigma/\Pi}}{R^8}+V_{exch}^{\Sigma/\Pi}, \tag{2}$$

where $V_{exch}^{\Sigma/\Pi}$ is the exchange energy between the two atoms, which is evaluated according to analytical formulas given in Ref. [18], and summarized in the Appendix for clarity. The exchange energy mainly depends on the product $a_{6s}a_{6p}$ of the asymptotic amplitudes of the $6s$ and $6p$ atomic wave functions. The $C_3^{\Sigma/\Pi}$ coefficients are related to the squared atomic transition dipole moment $M^2=|\langle 6s|r|6p\rangle|^2$, according to

$$C_3^{\Pi}=-\frac{C_3^{\Sigma}}{2}=-\frac{M^2}{3}=-\frac{3\hbar}{4\tau_{6p-6s}}\left(\frac{\lambda}{2\pi}\right)^3, \tag{3}$$

where $\lambda=2\pi\lambda\!\!\!^{-}$ is the wavelength of the $6s\rightarrow 6p$ atomic transition, and τ_{6p-6s} the corresponding radiative lifetime.

In Ref. [11], Gutterres *et al.* introduced for the first time into this type of analysis a weak variation of the spin-orbit coupling with the internuclear distance, which was found essential for the quality of the model. Such a variation is expected to be strong for Cs_2, as the $0_g^-(P_{3/2})$ external potential well lies at smaller distance than in Rb_2, i.e., in a region where the mixing with neighboring atomic configurations is expected to be important. This is confirmed by quantum chemistry calculations [19], reproduced in Fig. 1. As we look for an analytical expression for the $0_g^-(P_{3/2})$ external

potential well, we found that these numerical data can be conveniently represented by an analytical form beyond 8 Å:

$$\Delta^{\Pi\Pi}(R)=\frac{\Delta E_{FS}}{3}\tanh(\mathcal{A}^{\Pi\Pi}R), \tag{4}$$

$$\Delta^{\Pi\Sigma}(R)=\frac{\sqrt{2}\Delta E_{FS}}{3}\tanh(\mathcal{A}^{\Pi\Sigma}R), \tag{5}$$

where $\Delta E_{FS}=554.039\ \mathrm{cm}^{-1}$ is the Cs fine structure splitting. Calculations of Ref. [19] are nicely reproduced with $\mathcal{A}^{\Pi\Sigma}=0.217\ 955\ \text{Å}^{-1}$ and $\mathcal{A}^{\Pi\Pi}=0.219\ 023\ \text{Å}^{-1}$.

As cesium is a heavy atom, we include into Eqs. (1) and (2) other corrections accounting for relativistic effects. First, retardation effects are introduced through the correction factor $f^{\Sigma/\Pi}$ [20,21], multiplying the $C_3^{\Sigma/\Pi}/R^3$ term in Eq. (2):

$$f^{\Sigma}=\cos\left(\frac{R}{\lambda}\right)+\left(\frac{R}{\lambda}\right)\sin\left(\frac{R}{\lambda}\right)+\left(\frac{R}{\lambda}\right)^2\cos\left(\frac{R}{\lambda}\right), \tag{6}$$

$$f^{\Pi}=\cos\left(\frac{R}{\lambda}\right)+\left(\frac{R}{\lambda}\right)\sin\left(\frac{R}{\lambda}\right). \tag{7}$$

Second, in the above nonrelativistic model, the squared transition moments $(M_{3/2}^{nr})^2=|\langle 6s|r|6p_{3/2}\rangle|^2$ and $(M_{1/2}^{nr})^2=|\langle 6s|r|6p_{1/2}\rangle|^2$ for the $6s\rightarrow 6p_{3/2}$ and $6s\rightarrow 6p_{1/2}$ transitions, respectively, depend on M^2 through the simple relations

$$(M_{3/2}^{nr})^2=\frac{9\hbar}{2\tau_{3/2}}\left(\frac{\lambda_{3/2}}{2\pi}\right)^3=\frac{4}{3}M^2, \tag{8}$$

$$(M_{1/2}^{nr})^2=\frac{9\hbar}{4\tau_{1/2}}\left(\frac{\lambda_{1/2}}{2\pi}\right)^3=\frac{2}{3}M^2, \tag{9}$$

where $(\lambda_{3/2})^{-1}=11\ 732.3071\ \mathrm{cm}^{-1}$ and $(\lambda_{1/2})^{-1}=11\ 178.2682\ \mathrm{cm}^{-1}$ are the $6p_{3/2,1/2}\rightarrow 6s$ transition wave numbers [22,23], and $\tau_{3/2,1/2}$ the associated radiative lifetimes. In such expressions, the difference between radiative lifetimes arises from the transition wave number only, i.e., $\tau_{3/2}/\tau_{1/2}=\lambda_{1/2}^3/\lambda_{3/2}^3$. They do not include the modification of the atomic wave functions $6p_{3/2}$ and $6p_{1/2}$ due to the spin-orbit coupling, which can be introduced as a small correction through an effective parameter ϵ in the ratio of relativistic transition moments (see, for example, Ref. [24]):

$$\mathcal{R}=\frac{M_{3/2}^2}{M_{1/2}^2}=\frac{2\tau_{1/2}\lambda_{3/2}^3}{\tau_{3/2}\lambda_{1/2}^3}=\frac{2}{(1+\epsilon)^2}. \tag{10}$$

The final expression for the Hamiltonian in Hund's case *a* can be obtained by applying back and forth the transformation matrix $T_{a\rightarrow e}$ from Hund's case *a* to Hund's case *e*, which in the present case is

$$T_{a\rightarrow e}=\begin{pmatrix}\frac{1}{\sqrt{3}} & \sqrt{\frac{2}{3}}\\ \sqrt{\frac{2}{3}} & -\frac{1}{\sqrt{3}}\end{pmatrix}. \tag{11}$$

Defining $C_3^{\Pi}=-M_{3/2}^2/4$, and combining with Eq. (3), we obtain

$$V^{\Sigma}=\frac{-C_3^{\Sigma}}{R^3}\left(1+\frac{2\epsilon}{3}\right)-\frac{C_6^{\Sigma}}{R^6}-\frac{C_8^{\Sigma}}{R^8}+V_{exch}^{\Sigma}, \tag{12}$$

$$V^{\Pi}=\frac{-C_3^{\Pi}}{R^3}\left(1+\frac{4\epsilon}{3}\right)-\frac{C_6^{\Pi}}{R^6}-\frac{C_8^{\Pi}}{R^8}+V_{exch}^{\Pi}, \tag{13}$$

and

$$H=\begin{pmatrix}V^{\Pi}(R)-\Delta^{\Pi\Pi}(R) & \frac{\sqrt{2}}{9}\frac{M^2\epsilon}{R^3}+\Delta^{\Sigma\Pi}(R)\\ \frac{\sqrt{2}}{9}\frac{M^2\epsilon}{R^3}+\Delta^{\Sigma\Pi}(R) & V^{\Sigma}(R)\end{pmatrix}. \tag{14}$$

The diagonalization of the 2×2 matrix in Eq. (14) yields an analytical expression for the potential energy of the $0_g^-(P_{3/2})$ external well. Vibrational energies and wave functions are then calculated using a standard Numerov integration procedure. The rotational energy $E^{rot}(v,J)$ of a rovibrational level (v,J) can be estimated by the diagonal part of the rotational Hamiltonian $H^{rot}=[\mathbf{J}^2-2\mathbf{Jj}+\mathbf{j}^2]/(2\mu R^2)$, where $\mathbf{J}$ and $\mathbf{j}$ are the total angular momentum and the total electronic angular momentum, respectively, and μ the reduced mass of the system [8]:

$$E^{rot}(v,J)=\left\langle v\left|\frac{\hbar^2}{2\mu R^2}[J(J+1)+j(j+1)-2J_z\Omega]\right|v\right\rangle, \tag{15}$$

with $\Omega=0$ in the present case. The $0_g^-(P_{3/2})$ and $0_g^-(P_{1/2})$ states are asymptotically correlated to $j=2$ and $j=0$, respectively. The $[j(j+1)]$ term represents the rotational correction to the $J=0$ state, accounting for the internal structure of the atoms. It brings an energy contribution of $\delta E_0^{rot}=j(j+1)B_v$, i.e., at most $\delta E_0^{rot}=6B_v$, where $B_v=\langle v|(\hbar^2/2\mu R^2)|v\rangle$ is the rotational constant.

In the following section, we determine the potential energy of the $0_g^-(P_{3/2})$ external well by varying the following set $\{p_i\}$ of $N_p=9$ parameters: the squared atomic transition dipole moment M^2, the van der Waals parameters $C_6^{\Sigma/\Pi}$, $C_8^{\Sigma/\Pi}$, the product $a_{6s}a_{6p}$, the amplitude for spin-orbit coupling terms $\mathcal{A}^{\Pi\Sigma}$, $\mathcal{A}^{\Pi\Pi}$, and the relativistic parameter ϵ. The retardation functions $f^{\Sigma/\Pi}$ are kept fixed to their value of Refs. [20,21].

III. THE ASYMPTOTIC PARAMETERS OF THE $Cs_2\ 0_g^-(P_{3/2})$ EXTERNAL WELL

The rovibrational energies $E(v,J)$ of the $0_g^-(P_{3/2})$ levels calculated within the framework of the model above are adjusted to the experimental values E_{vJ}^{exp} previously presented in paper I, recorded with an absolute accuracy of $\pm 0.005\ cm^{-1}$. All transition energies in Ref. [15] are measured relative to the $6S_{1/2}(F=4)+6S_{1/2}(F=4)$ and $6S_{1/2}(F=4)+6P_{3/2}(F=5)$ energy difference, where F is the total angular momentum of the atom. As we do not include hyperfine structure in our model, we substract $0.0088\ cm^{-1}$ from all experimental energies, to relate them to the barycenter of the $6S_{1/2}(F=4)+6P_{3/2}$ manifold.

In order to obtain the best possible fit, we restricted the experimental dataset to the 75 lowest vibrational levels from $v=0$ to $v=74$, over the 133 levels measured, and to the rotational level $J=2$, which corresponds to the by far most intense line of the observed rotational progressions involving $J=0$–6. Beyond $v=74$, the rotational lines are no longer separated in the spectrum and the hyperfine structure becomes significant. Moreover, such a restriction removes a need to take account of the top of the potential barrier, around $15a_0$, separating the external well from the inner well, whose shape is strongly influenced by the large exchange interaction.

The optimization procedure minimizes the root-mean-squared (rms) deviation:

$$\mathrm{rms}=\frac{1}{N_p-N}\sqrt{\sum_{i=1}^{N}[E_{vJ}^{exp}-E_{vJ}(\{p_i\})]^2}. \qquad (16)$$

As in paper I, we used a minimization procedure based on the so-called generalized simulated annealing (GSA) method, which is easy to handle for nonlinear fits of the long-range behavior of molecular potentials (see Refs. [26,25], and references therein). Initial values for M^2 and ϵ are deduced from available measurements of atomic lifetimes [27], and from Refs. [28,18] for the remaining parameters. We choose also for beginning the upper bound $\delta E_0^{rot}=6B_v$.

In our best fit, the experimental energy levels lying in the $0_g^-(P_{3/2})$ external well are reproduced with a rms of $0.0065\ cm^{-1}$, close to the accuracy of the experimental measurements, and Table I presents the asymptotic parameters obtained from this analysis. Values for M^2, $C_6^{\Sigma/\Pi}$, and C_8^{Π} parameters are in good agreement with the theoretical predictions (with a relative difference smaller than 5%). As in paper I, the discrepancy in the C_8^{Σ} parameter is the largest of all parameters, but still satisfactory. In contrast, the exchange parameter $a_{6s}a_{6p}$ is two times smaller than the initial value derived from Ref. [18], which suggests that the asymptotic exchange energy is probably overestimated in this latter work (see the Appendix).

The effective R dependence of the spin-orbit coupling has an important role in the adjustment, as illustrated in Table I. Without such a variation, the experimental energies are reproduced by our model with a larger rms of $0.009\ cm^{-1}$. Figure 1 shows a plot of the $\Delta^{\Pi\Pi}(R)$ and $\Delta^{\Sigma\Pi}(R)$ effective spin-orbit coupling obtained in the present work, compared to calculated results of Ref. [19]. The agreement between both representations of the spin-orbit coupling is very satisfactory in the long-range region. For $R\approx 10$ Å the discrepancies between our results and the *ab initio* calculations are more important but still compatible with the expected uncertainty of the theoretical results. Indeed, in a recent work on analysis of predissociation width in the $0_u^+(6S+6P_{3/2})$ photoassociation spectra above the $(6S+6P_{1/2})$ dissociation limit [29], Kokoouline *et al.* have shown that *ab initio* calculations of Ref. [19] overestimate the decrease of the spin-orbit coupling when the internuclear distance is decreasing.

TABLE I. Asymptotic parameters for the $Cs_2\ 0_g^-(P_{3/2})$ state obtained in the present work: (i) our best fit, with all parameters free, (ii) with $\mathcal{A}^{\Pi\Sigma}=\mathcal{A}^{\Pi\Pi}=0$. The standard deviations in the last significant digit of the parameters, indicated in parentheses, are deduced from the statistical analysis of a series of fits performed on artificial experimental energies (see text). Values in square brackets are kept fixed during the fit [case (ii)].

Parameter	This work	Other results
M^2 ($10^5\ cm^{-1}$ Å^3)	(i) 9.7890(1) (ii) 9.7856	10.22 [28]
$C_6(^3\Pi_g)$($10^7\ cm^{-1}$ Å^6)	(i) 5.689(1) (ii) 5.668	5.701(1) [28]
$C_6(^3\Sigma_g)$($10^7\ cm^{-1}$ Å^6)	(i) 8.506(1) (ii) 8.773	8.381(1) [28]
$C_8(^3\Pi_g)$($10^9\ cm^{-1}$ Å^8)	(i) 3.180(3) (ii) 3.093	3.045(3) [28]
$C_8(^3\Sigma_g)$($10^{-9}\ cm^{-1}$ Å^8)	(i) 7.715(3) (ii) 9.374	6.802(3) [28]
$a_{6s}a_{6p}$	(i) 0.038 433(3) (ii) 0.038 430	0.054 790 [18]
$\mathcal{A}^{\Pi\Sigma}$ (Å^{-1})	(i) 0.2661(5) (ii) [0]	
$\mathcal{A}^{\Pi\Pi}$ (Å^{-1})	(i) 0.2413(2) (ii) [0]	
ϵ (units of 10^{-3})	(i) 4.69(3) (ii) [4.69]	
rms (cm^{-1})	(i)0.0065 (ii) 0.0090	

The exchange energy determined by $a_{6s}a_{6p}$ has a negligible contribution over most of the potential well. It starts to be noticeable (say, larger than the rms of the fit) below 17 Å, corresponding to the outer turning point of the $v=17$ level. It then increases exponentially to reach 1% of the potential energy at the equilibrium distance, and about 15% at the inner turning point of the uppermost level ($v=74$) included in the fit. The perturbative treatment of the exchange energy is then valid. The other corrections are even smaller: the retardation term increases slowly from $0.001\ cm^{-1}$ around 100 Å, up to $0.008\ cm^{-1}$ at the equilibrium distance. We checked also that decreasing the δE_0^{rot} below its upper bound $6B_v$ affects the rms of the adjustment by less than 1%, and

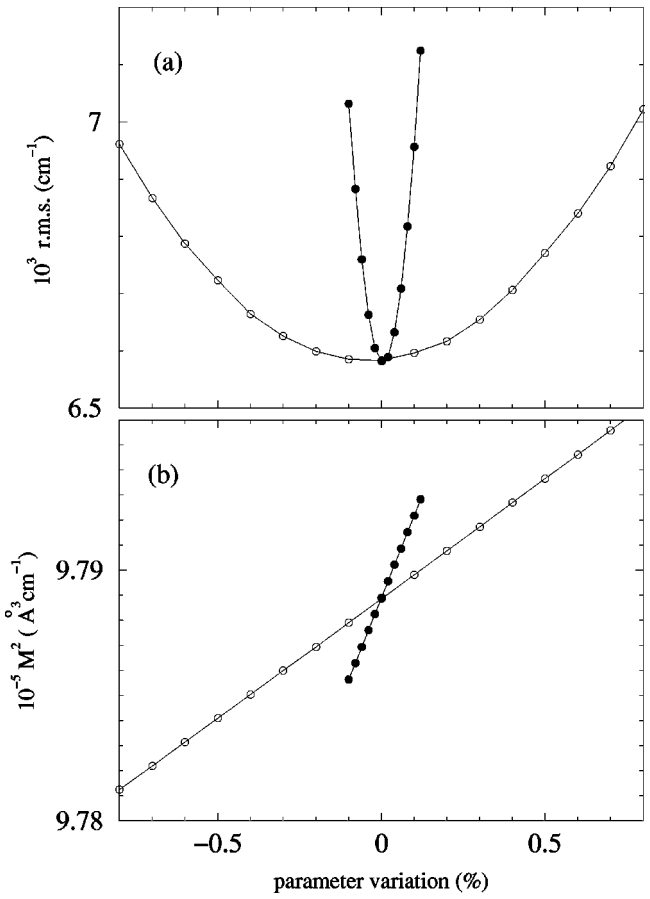

FIG. 2. Variation of the rms of the fit (a) and of M^2 (b) when C_6^{Π} (closed circles) and C_6^{Σ} (open circles) are varied individually.

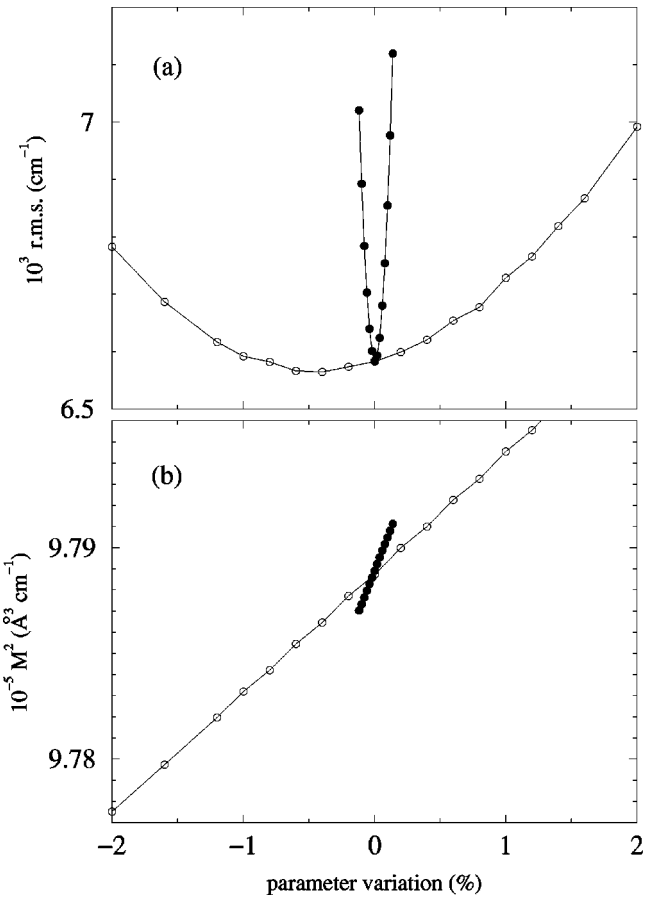

FIG. 3. Same as Fig. 2 for variation of C_8^{Π} (closed circles) and C_8^{Σ} (open circles).

the adjusted parameters by an amount well below the error bars discussed in the following section. The same conclusion applies when we include a term C_{10}/R^{10} in the multipolar expansion [Eq. (2)], or the nonadiabatic coupling operator d^2/dR^2.

IV. DISCUSSION

As discussed in previous papers, the GSA method does not yield a direct evaluation of the error on the fitted parameters, which in any case would not be meaningful due to their nonstatistical distribution.

We first proceed as in the Rb_2 study of Ref. [11], by analyzing the variation of M^2 when the other parameters are varied individually, and looking at the rms error behavior. As displayed on Figs. 2–4, our best fit corresponds indeed to a well-defined minimum of the rms, more or less pronounced depending on which parameter is varied. The fastest variation of the rms is found when C_6^{Π} and C_8^{Π} are changed by a few tenths of a percent (Figs. 2 and 3), reaching 0.007 cm^{-1}. In contrast, a similar increase of the rms is observed when C_6^{Σ} and C_8^{Σ} (Figs. 2 and 3), $\mathcal{A}^{\Pi\Pi}$, $\mathcal{A}^{\Pi\Sigma}$, and $a_{6s}a_{6p}$ (Fig. 4) are changed by $\approx 1\%$. The effective relativistic parameter ϵ has a very small influence over the rms for such variations. It is also remarkable that the present nonlinear fit results in all cases into linear variations of M^2 with all parameters, at least in the vicinity of the rms minimum.

Then the error of the fitted parameters can be estimated if we can rely on a satisfactory criterion to decide how well the minimum of the rms can be located in Figs. 2–4. In Ref. [11], a 10% variation of the rms provided an upper bound—probably largely overestimated—for the error on M^2. Here, we determine a standard deviation on the parameters by fitting 100 sets of artificial experimental energies, obtained after adding a random distribution of the experimental error bar (± 0.005 cm^{-1}) over the measured energies. The standard deviations reported in Table I are very small for all parameters, with an rms for each individual artificial set around 0.007 cm^{-1}. We also performed two further trials to check the internal consistency of our adjustments. First, we created artificial energy set by distributing the experimental error over the level energies calculated from our best fitted potential defined by the parameters in Table I. As expected, the rms is reduced down to 0.003 cm^{-1}. Second, we modified the level energies with a constant upward or downward shift of 0.005 cm^{-1}, providing a rms around 0.001 cm^{-1}.

The final error bar on the leading parameter, i.e., on the transition dipole moment M^2 has to take into account the probable limitations of our model. The various contributions already mentioned in the preceding section (i.e., the C_{10}/R^{10} term and the variation of the rotational energies) are respon-

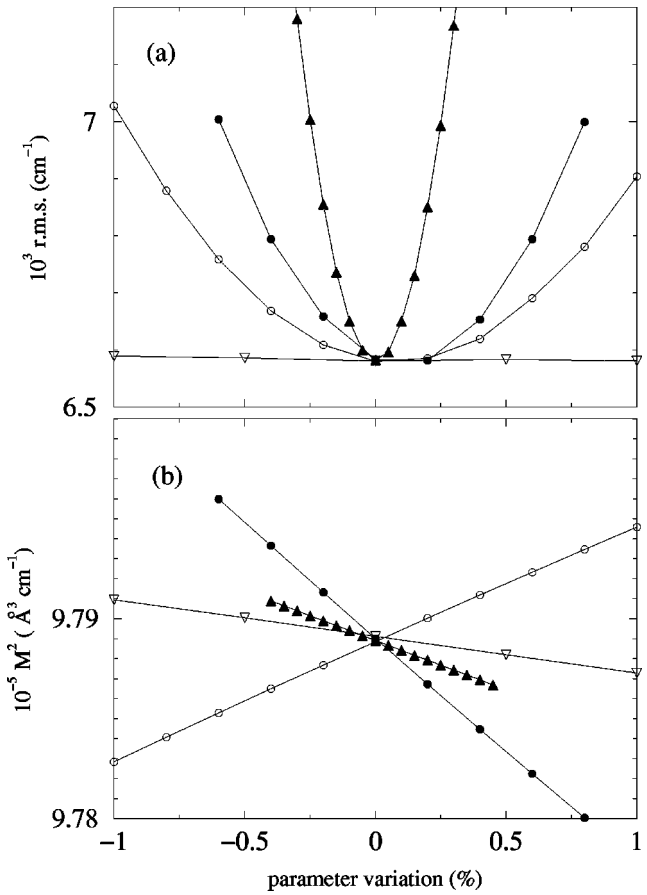

FIG. 4. Same as Fig. 2 for variation of $\mathcal{A}^{1\Pi}$ (closed circles), $\mathcal{A}^{1\Sigma}$ (open circles), $a_{6s}a_{6p}$ (closed triangles), and ϵ (open triangles).

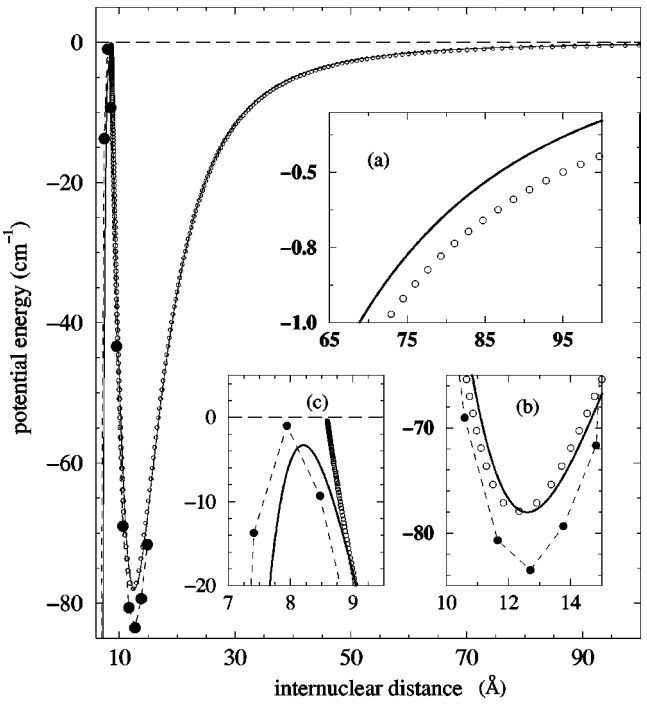

FIG. 5. Potential curve of the $0_g^-(P_{3/2})$ external well, obtained in the present work (full line) and from our previous RKR analysis [15] (open circles). The curve deduced from the quantum chemistry calculations of Ref. [19], and already displayed in Ref. [15], is recalled (closed circles). Insets emphasize differences between these various determinations (a) at large distances, (b) around the equilibrium distance, and (c) in the region of the barrier. The deviation from the expected R^{-3} long-range behavior of the RKR curve is clearly seen in inset (a).

sible for a variation of M^2 of about 20 cm^{-1} Å^3 and 30 cm^{-1} Å^3, respectively. The nonadiabatic term has no influence at this level of precision. Then we estimate that the cumulative effect of statistical error and error from neglected terms leads to an uncertainty on M^2 of ± 100 cm^{-1} Å^3, or 0.01%, which is about ten times smaller than in the recent determination of Ref. [10].

In Fig. 5 we draw the present analytical representation of the potential-energy curve and the RKR curve of paper I. On the global picture, both approaches agree each other, while the curve obtained from the quantum chemistry calculations of Ref. [19] has a well depth that is greater by only 5.4 cm^{-1}. However, important differences are visible in the insets, at both short and large distances. Indeed, whereas both the repulsive and the attractive branch of the $0_g^-(P_{3/2})$ external well manifest R^{-3} behavior, it is assumed in the standard RKR treatment that the short-range part of the potential well behaves as an exponential repulsive barrier [Fig. 5(c)], which in turn draws the long-range part of the curve away from a pure R^{-3} variation [Fig. 5(a)]. This is why it is not possible to fit a C_3 parameter to the RKR potential. The equilibrium distance $R_e = 12.60$ Å is larger than in the RKR approach ($R_e = 12.35$ Å), as suggested in Fig. 5(b). The well depth is also slightly increased to $D_e = 78.026$ cm^{-1}, compared to $D_e = 77.950$ cm^{-1} for the RKR curve. Rotational constants are also slightly affected (Fig. 6), yielding only a weak modification of the rotational energy levels, i.e., around 0.0004 cm^{-1} for $v = 0$, $J = 2$, and 0.0006 cm^{-1} for $v = 74$, $J = 2$. In short, the fitted RKR potential can be used as a tool to reproduce the measured vibrational energy levels, but not to deduce the fundamental physical quantities.

Another important issue concerns the scattering length of

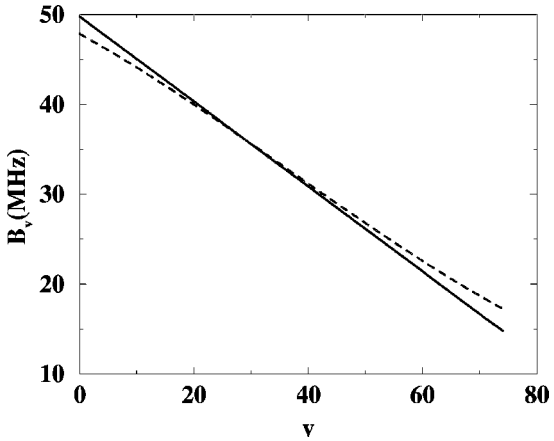

FIG. 6. Rotational constants for vibrational levels of the $0_g^-(P_{3/2})$ external well, obtained in the present work (dashed line) and from our previous RKR analysis [15] (full line).

TABLE II. Correspondence between the energy position (with measured uncertainties in parentheses) of the intensity minima of the cesium photoassociation spectrum of Ref. [1] and the outer turning points in the representations of the $0_g^-(P_{3/2})$ external well.

Intensity minimum	Detuning (cm^{-1})	R (Å) (This work)	R (Å) (Ref. [1])
2	−10.415(0.07)	31.19	31.22
3	−19.142(0.05)	25.21	25.19
4	−28.358(0.10)	21.84	21.75
5	−37.732(0.05)	19.57	19.47
6	−46.554(0.10)	17.95	17.83
7	−54.331(0.10)	16.74	16.56
8	−62.724(0.10)	15.56	15.35
9	−68.604(0.10)	14.73	14.50

the lowest triplet state in Cs_2, for which a value has been extracted recently using the PA data for the $0_g^-(P_{3/2})$ state [16]. Considering the energies of the intensity minima in the PA spectrum, the positions of the outer turning points for the corresponding vibrational levels are reported in Table II both for the RKR potential and for the analytical one. From the reflection approximation [30,31], such internuclear distances approximately correspond to the nodes in the scattering wave function describing collisions of two cold cesium atoms along the $a^3\Sigma_u^+$ potential. When moving from the outer to the inner nodes, shifts of 0.03–0.23 Å are manifested, the node position being sytematically located at larger internuclear distances when the analytical potential is considered. Such shifts should have significant consequences on the determination of the scattering length.

The most important result of the present work is the determination of the lifetime of the $6P_{3/2}$ and $6P_{1/2}$ atomic levels, which are derived from Eq. (3) using the atomic transition frequencies of $6S_{1/2}-6P_{1/2}$ and $6S_{1/2}-6P_{3/2}$ from Refs. [22,23]. Our value for $\tau_{3/2}$, reported in Table III and in Fig. 7, together with other recent determinations, presents an accuracy (0.01%) improved by at least one order of magnitude compared to the previous experimental values. Our value for $\tau_{1/2}$ has also an improved accuracy (0.06%), limited by the uncertainty on the measured lifetime ratio $\mathcal{R}$ (0.01%). In particular, both lifetimes lie within the error bar of the pulsed laser measurements of Ref. [32], whereas it is outside the error bar of the measurements using laser excitation of a fast atomic beam [27]. This conclusion is in agreement with the recent theoretical determination of Derevianko and Porsev [10]. These authors deduce the squared electric dipole moment $M_{1/2}^2$ for the $6P_{1/2}\rightarrow 6S_{1/2}$ transition from the van der Waals coefficient C_6^{6s} of the Cs_2 ground state. Their 0.1% error bar on $M_{1/2}^2$ is mainly constrained by the uncertainty on the C_6^{6s} coefficient. The electric dipole moment for the $6P_{3/2}\rightarrow 6S_{1/2}$ transition is then obtained from the ratio $\mathcal{R}$ of Eq. (10), and measured in Ref. [33] with a precision of 0.05%. We note from Table III that the present determination of $\mathcal{R}$ lies within the error bar of Ref. [33]. Using $C_6^{6s}=6859(25)$ a.u., as deduced from ultracold atomic collisions [14], the method of Derevianko and Porsev leads to a lifetime $\tau_{3/2}=30.39\pm0.06$ ns, so that the present determination lies just outside the error bar. However, two of us recently determined from Fourier-transform spectroscopy (FTS) a value $C_6^{6s}=6836(100)$ a.u. [34]. Reporting the central value $C_6^{6s}=6836$ a.u. in formula (9) of Ref. [10], we obtain a new lifetime that is compatible with the present determination (see dashed line in Fig. 7).

TABLE III. Radiative lifetime of the $6P_{3/2}$ and $6P_{1/2}$ Cs states resulting from the present analysis. Numbers in italics are deduced from quoted original papers. The error in $\tau_{3/2}$ results from the cumulative effect of statistical or systematic errors detailed in the text. The $\tau_{1/2}$ lifetime is deduced either by using the $\mathcal{R}$ from our fit (i) or from the experiment of Ref. [33] (ii).

	$\tau_{3/2}$ (ns)	$\tau_{1/2}$ (ns)	$\mathcal{R}$	$\epsilon\times10^3$
Present work	30.462(3)	(i) 34.89(2)	1.9814(11)	4.69
		(ii) 34.88(2)		
Ref. [10]	30.39(6)	34.80(7)	1.9809(84)	4.8
Ref. [27]	30.57(7)	35.07(10)	1.9844(103)	3.9
Ref. [33]			1.9809(9)	4.8
Ref. [32]	30.41(10)	34.75(7)		5.8

Moreover, we can use the method of Ref. [10] to deduce a C_6^{6s} coefficient of the ground state from the present fitted C_3 value. Derevianko and Porsev write

$$C_6^{6s}=M_{1/2}^4\xi_p+M_{1/2}^2\xi_x+\xi_r, \tag{17}$$

where ξ_p, ξ_x, and ξ_r are coefficients evaluated by these authors. From our value of $\tau_{3/2}$, we can derive $M_{3/2}$, and then derive $M_{1/2}$ using our $\mathcal{R}$ value. This gives finally $C_6^{6s}=6828(19)$ a.u., in agreement with the FTS value above, and with the value by Leo *et al.* [14]. The error bar is estimated by considering the uncertainties on the ξ_p, ξ_x, and ξ_r parameters reported in Ref. [10], and the one on $\mathcal{R}$ from our analysis. Using the $\mathcal{R}$ value of Ref. [33] leads to a similar conclusion. Then the improvement of the determination of

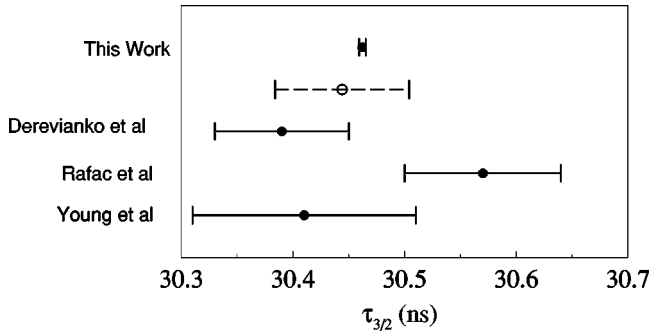

FIG. 7. Present value and error bar of the lifetime for the $6P_{3/2}$ level of the cesium atom, compared to the experimental result of Young *et al.* [32] and Rafac *et al.* [27], and to the theoretical determination of Derevianko and Porsev [10] involving $C_6^{6s}=6859(25)$ a.u. [14]. Using the value $C_6^{6s}=6836$ a.u. from Ref. [34], implemented within the method of Ref. [10], yields a lifetime in agreement with the present value, and is represented by the dashed line.

the $\tau_{3/2}$ lifetime allowed to obtain a 0.3% accuracy for C_6^{6s}, now limited by the precision of the $\mathcal{R}$ measurement.

V. CONCLUSION

The extraction of an analytical representation for the Cs_2 long-range potentials from photoassociation spectra is important for the determination of data such as atomic lifetimes or scattering lengths. Till very recently, it seemed that in contrast with the lighter alkali dimers, the task was impossible for Rb_2 and Cs_2. Following a method already implemented for Rb_2 [11], we have proposed a determination of the external well in the Cs_2 $0_g^-(P_{3/2})$ double-well potential curve by fitting the parameters of a two-state model Hamiltonian, involving the long-range expansion of the $^3\Pi_g(6s+6p)$ and $^3\Sigma_g^+(6s+6p)$ potential curve and a fine-structure coupling term for which we considered an explicit R dependence. Small corrections for asymptotic exchange term and relativistic effects are also included. The experimental data are the levels v, $J=2$ corresponding to the most accurate lines in the photoassociation spectrum of Ref. [15], with v varying from 0 to 74, in an energy region where hyperfine-structure effects can safely be neglected. As in previous work [11], we use the generalized simulated annealing method for the fit. The error checks are performed either by modifying individually each parameter to verify that the best fit corresponds indeed to a well-defined minimum, or by fitting sets of artificial experimental energies modified with random distribution of the experimental error bar. Including an estimation of possible missing effects in the model leads to an uncertainty as small as 0.01% on the leading parameter M^2, where M is the electric dipole moment for the transition $6P_{3/2}\rightarrow 6S_{1/2}$ in the cesium atom. This suggests that the present method could provide lifetimes for the cesium atom with an accuracy better than any other determination.

Important differences between the curve obtained using the present asymptotic approach and a previous RKR determination [15] from the same set of data were found and discussed. They can be justified by the hypothesis, in the standard RKR treatment, of an exponential behavior of the potential curves at short range, which overlooks the characteristic shape of the present well, where both the inner and the outer branches display a typical R^{-3} behavior, so that they should not be modified independently. This explains why from the RKR fit in Ref. [15] it was impossible to extract a C_3 coefficient. Present results have strong consequences in the determination of Cs_2 $0_g^-(P_{3/2})$ wave functions and in the derivation of the Cs_2 $^3\Sigma_u^+$ lower triplet state scattering length.

Whereas the $Cs(6P_{3/2})$ radiative lifetime can be extracted from photoassociation spectra with an accuracy better than in atomic experiments, we obtain the $Cs(6P_{1/2})$ lifetime with an accuracy equivalent to previous works. The performed analysis allows the direct evaluation of relativistic effects, inducing the difference between the $S\rightarrow P_{1/2}$ and $S\rightarrow P_{3/2}$ transition matrix elements. The values obtained for the lifetimes are $\tau_{3/2}=30.462(3)$ ns and $\tau_{1/2}=34.88(2)$ ns, in agreement with pulsed laser measurements of Young *et al.* [32]. They are compared with a recent theoretical determination of Derevianko and Porsev [10] computed from a value of the ground state C_6^{6s} coefficient deduced from ultracold atom-atom collision experiments [14]. The agreement is good, and it becomes excellent when a C_6^{6s} value fitted on Fourier-transform molecular spectroscopy is used. The agreement between two independent theoretical determinations strongly supports the present analysis. Finally, the small error bar of the present determination of the electric dipole moment for the transition $6P_{1/2}\rightarrow 6S_{1/2}$ is used to extract a $C_6^{6s}=6828(19)$ a.u. coefficient for the Cs_2 ground state, in good agreement with Ref. [14].

ACKNOWLEDGMENTS

We thank the experimental cold molecule group of Pierre Pillet for stimulating discussions, as well as Eberhard Tiemann, Christian Lisdat, and Andrei Derevianko. Thanks are also due to Daniel Comparat for discussions on the treatment of statistical errors. Laboratoire Aimé Cotton is associated with Université Paris Sud, Orsay. A critical reading of the manuscript by Professor R. J. Le Roy was very much appreciated.

APPENDIX: EXPRESSION OF THE EXCHANGE ENERGY

We recall here the main equations of Ref. [18], using the notations therein, in order to clarify the parameters involved in the fitting procedure. The asymptotic exchange energy $V_{exch}^{\Sigma/\Pi}$ for the $^3\Sigma_g^+$ and $^3\Pi_g$ states correlated to the $6s+6p$ dissociation limit of Cs_2 is expressed as

$$V_{exch}^{\Sigma/\Pi}=I_{no}-I_{ex}, \tag{A1}$$

where I_{no} and I_{ex} are the exchange integrals without and with excitation transfer, respectively. They are calculated by considering the asymptotic behavior of the normalized atomic wave functions ϕ_{6s} and ϕ_{6p}:

$$\phi_{6s}\approx a_{6s}r^{1/\alpha-1}e^{-\alpha r}, \tag{A2}$$

$$\phi_{6p}\approx a_{6p}r^{1/\beta-1}e^{-\beta r}, \tag{A3}$$

where $\alpha=\sqrt{-2E_{6s}}$ and $\beta=\sqrt{-2E_{6p}}$ are fixed quantities related to the binding energies E_{6s} and E_{6p} of the $6s$ and $6p$ levels, and a_{6s} and a_{6p} are the asymptotic amplitudes of the wave functions. The formal expression for I_{no} and I_{ex} is written as

$$I_{no}=-(a_{6s}a_{6p})^2\mathcal{C}_{no}R^{\gamma-m}e^{-\mu R}J_m(R), \tag{A4}$$

$$I_{ex}=-(a_{6s}a_{6p})^2\mathcal{C}_{ex}R^{\gamma-m}e^{-\mu R}, \tag{A5}$$

where R is the interatomic distance; $m=0$ and 1 for the Σ and Π states, respectively. The complete expressions for the integral expression $J_m(R)$, and for the coefficients $\mathcal{C}_{no}$, $\mathcal{C}_{ex}$, γ, and μ are presented in Ref. [18], and are not given here. Let us note, however, that Eq. (5.13) of that paper contains a few typographical errors in the exponents of three factors,

which,after checking with the authors, should read $(2\alpha/\mu)^{(-1-1/\beta)}$, $(2\beta/\mu)^{(-1-1/\alpha)}$, and $(2\mu)^{(-2-1/\mu-m)}$.

In the expressions above, a_{6s} and a_{6p} are the only parameters that depend on the accuracy of the atomic wavefunction determinations. In Ref. [18], their value for cesium are $a_{6s}=0.510\ 20$ and $a_{6p}=0.107\ 39$. In the present work, the product $a_{6s}a_{6p}$ is considered as a fitting parameter, with the initial value 0.054 79. Let us note that another calculation [35] yields $a_{6s}=0.42$, which would reduce the product $a_{6s}a_{6p}$ to 0.045 10, assuming the same value for a_{6p}.

[1] A. Fioretti, D. Comparat, A. Crubellier, O. Dulieu, F. Masnou-Seeuws, and P. Pillet, Phys. Rev. Lett. **80**, 4402 (1998).

[2] A. N. Nikolov, E. E. Eyler, X. T. Wang, J. Li, H. Wang, W. C. Stwalley, and P. L. Gould, Phys. Rev. Lett. **82**, 703 (1999).

[3] C. Gabbanini, A. Fioretti, A. Lucchesini, S. Gozzini, and M. Mazzoni, Phys. Rev. Lett. **84**, 2814 (2000).

[4] D. Comparat, C. Drag, A. Fioretti, O. Dulieu, and P. Pillet, J. Mol. Spectrosc. **195**, 229 (1999).

[5] W. C. Stwalley, Y. H. Uang, and G. Pichler, Phys. Rev. Lett. **41**, 1164 (1978).

[6] W. I. McAlexander, E. R. I. Abraham, and R. G. Hulet, Phys. Rev. A **54**, R5 (1996).

[7] K. M. Jones, P. S. Julienne, P. D. Lett, W. D. Phillips, E. Tiesinga, and C. J. Williams, Europhys. Lett. **35**, 85 (1996).

[8] H. Wang, J. Li, X. T. Wang, C. J. Williams, P. L. Gould, and W. C. Stwalley, Phys. Rev. A **55**, R1569 (1997).

[9] U. Volz and H. Schmoranzer, Phys. Scr. **T65**, 48 (1996).

[10] A. Derevianko and S. G. Porsev, Phys. Rev. A **65**, 053403 (2002).

[11] R. F. Gutterres, C. Amiot, A. Fioretti, C. Gabbanini, M. Mazzoni, and O. Dulieu, Phys. Rev. A **66**, 024502 (2002).

[12] M. A. Bouchiat and C. Bouchiat, Rep. Prog. Phys. **60**, 1351 (1997).

[13] S. C. Bennet and C. E. Wieman, Phys. Rev. Lett. **82**, 2484 (1999).

[14] P. J. Leo, E. Tiesinga, C. J. Williams, and P. S. Julienne (unpublished).

[15] A. Fioretti, D. Comparat, C. Drag, C. Amiot, O. Dulieu, F. Masnou-Seeuws, and P. Pillet, Eur. Phys. J. D **5**, 389 (1999).

[16] C. Drag, B. Laburthe Tolra, B. T'Jampens, D. Comparat, M. Allegrini, A. Crubellier, and P. Pillet, Phys. Rev. Lett. **85**, 1408 (2000).

[17] B. Ji, C. C. Tsai, and W. C. Stwalley, Chem. Phys. Lett. **236**, 242 (1995).

[18] M. Marinescu and A. Dalgarno, Z. Phys. D: At. Mol. Clusters **36**, 239 (1996).

[19] N.Spiess, Ph.D thesis, Fachbereich Chemie, Universität Kaiserslautern, 1989 (unpublished).

[20] R. McLone and E. Power, Mathematika **11**, 91 (1964).

[21] W. J. Meath, J. Chem. Phys. **48**, 227 (1968).

[22] Th. Udem, J. Reichert, R. Holzwarth, and T. W. Hansch, Phys. Rev. Lett. **82**, 3568 (1999).

[23] Th. Udem, J. Reichert, T. W. Hansch, and M. Kourogi, Phys. Rev. A **62**, 031801 (2000).

[24] D. Comparat, Ph.D. thesis, Université Paris-Sud-Orsay, 1999 (unpublished).

[25] R. F. Gutteres, M. Argollo de Menezes, C. E. Fellows, and O. Dulieu, Chem. Phys. Lett. **300**, 131 (1999).

[26] C. E. Fellows, R. F. Gutterres, A. P. C. Campos, J. Vergès, and C. Amiot, J. Mol. Spectrosc. **197**, 19 (1999).

[27] R. J. Rafac, C. E. Tanner, A. E. Livingston, and H. G. Berry, Phys. Rev. A **60**, 3648 (1999).

[28] M. Marinescu and A. Dalgarno, Phys. Rev. A **52**, 311 (1995).

[29] V. Kokoouline, C. Drag, P. Pillet, and F. Masnou-Seeuws, Phys. Rev. A **65**, 062710 (2002).

[30] A. Jablonski, Phys. Rev. **68**, 78 (1945).

[31] P. S. Julienne, J. Res. Natl. Inst. Stand. Technol. **101**, 487 (1996).

[32] L. Young, W. T. Hill, III, S. J. Sibener, S. D. Price, C. E. Tanner, C. E. Wieman, and S. R. Leone, Phys. Rev. A **50**, 2174 (1994).

[33] R. J. Rafac and C. E. Tanner, Phys. Rev. A **58**, 1087 (1998).

[34] C. Amiot and O. Dulieu, J. Chem. Phys. **117**, 5155 (2002).

[35] A. V. Evseev, A. A. Radtsig, and B. M. Smirnov, Opt. Spectrosc. **44**, 495 (1978).